European Journal of Pharmaceutical Sciences 161 (2021) 105778

Contents lists available at ScienceDirect

European Journal of Pharmaceutical Sciences

journal homepage: www.elsevier.com/locate/ejps

Exploring porcine gastric and intestinal fluids using microscopic and solubility estimates: Impact of placebo self-emulsifying drug delivery system administration to inform bio-predictive *in vitro* tools

Harriet Bennett-Lenane [a], Jacob R. Jørgensen [b], Niklas J. Koehl [a], Laura J. Henze [a], Joseph P. O'Shea [a], Anette Müllertz [b], Brendan T. Griffin [a,*]

[a] School of Pharmacy, University College Cork, Cork, Ireland
[b] Department of Pharmacy, University of Copenhagen, Universitetsparken 2, 2100 Copenhagen Ø, Denmark

ARTICLE INFO

Keywords:
Landrace pigs
Oral drug delivery
In vitro tools
Bio-enabling formulations

ABSTRACT

Validation and characterisation of *in vitro* and pre-clinical animal models to support bio-enabling formulation development is of paramount importance. In this work, *post-mortem* gastric and small intestinal fluids were collected in the fasted, fed state and at five sample-points post administration of a placebo Self-Emulsifying Drug Delivery System (SEDDS) in the fasted state to pigs. Cryo-TEM and Negative Stain-TEM were used for ultra-structure characterisation. *Ex vivo* solubility of fenofibrate was determined in the fasted-state, fed-state and post-SEDDS administration. Highest observed *ex vivo* drug solubility in intestinal fluids after SEDDS administration was used for optimising the biorelevant *in vitro* conditions to determine maximum solubility. Under microscopic evaluation, fasted, fed and SEDDS fluids resulted in different colloidal structures. Drug solubility appeared highest 1 hour post SEDDS administration, corresponding with presence of SEDDS lipid droplets. A 1:200 dispersion of SEDDS in biorelevant media matched the highest observed *ex vivo* solubility upon SEDDS administration. Overall, impacts of this study include increasing evidence for the pig preclinical model to mimic drug solubility in humans, observations that SEDDS administration may poorly mimic colloidal structures observed under fed state, while microscopic and solubility porcine assessments provided a framework for increasingly bio-predictive *in vitro* tools.

1. Introduction

Trends in physicochemical properties of molecules in drug development pipelines continuously display an increasing prevalence of poorly water soluble drugs (PWSD) (1, 2). Resultantly, the pharmaceutical industry must adapt to ensure developability of such candidates. Solubility in the gastrointestinal tract (GIT) is an important parameter in guiding the oral developability classification, as previous estimates suggest approximately 40% of new chemical entities are rejected in early development owing to insufficient solubility (3). Prevalence of such challenging properties provokes a multifaceted response; including development of bio-enabling formulations, in addition to both development and validation of *in vitro* tools and pre-clinical animal models to accurately forecast *in vivo* behaviour, together counteracting increasing product attrition.

One common bio-enabling formulation strategy involves the use of self-emulsifying drug delivery systems (SEDDS) (4). SEDDS are a type of lipid-based formulation (LBF) composed of an isotropic mixture of oils, surfactants and co-solvents, designed to self-emulsify following dispersion within the GIT. SEDDS include various mixtures of lipophilic and/or hydrophilic surfactants, helping to emulate positive food effects experienced by many PWSD, as concentrations of bile salts and phospholipids

Abbreviations: PWSD, Poorly Water-Soluble Drug; LBF, Lipid-Based Formulations; SEDDS, Self-emulsifying drug delivery systems; GIT, Gastrointestinal tract; DCS, Developability Classification System; BCS, Biopharmaceutics Classification System; TEM, Transmission Electron Microscopy; USI, Upper Small Intestine (Duodenum); MSI, Middle Small Intestine (Jejunum); LSI, Lower Small Intestine (Ileum); FaSSIF, Fasted State Simulated Intestinal Fluid; FaSSGF, Fasted State Simulated Gastric Fluids; FaSSIFp, Fasted State Simulated Intestinal Fluid of Pigs; FaHIF, Fasted State Human Intestinal Fluid; FeHIF, Fed State Human Intestinal Fluids; OrBiTo, Oral Biopharmaceutics Tools; SGFsp, Simulated Gastric Fluid without Pepsin.

* Corresponding author.
E-mail address: brendan.griffin@ucc.ie (B.T. Griffin).

https://doi.org/10.1016/j.ejps.2021.105778
Received 28 January 2021; Received in revised form 22 February 2021; Accepted 23 February 2021
Available online 26 February 2021

are increased in the fed state (5). These endogenous surfactants, in combination with lipid digestion products, may increase the solubilisation capacity in the GIT fluids for PWSD through creation of a range of colloidal structures. In this heterogeneous environment, the solubility deficit between the fasted and fed state can be bridged (6, 7).

Successful application of such bio-enabling oral drug delivery systems is often dependent on existence of efficacious screening processes and predictive *in vitro* models simulating the GIT. These investigations provide vital tools for progression of bio-enabling drug delivery systems, ideally simulating the likely *in vivo* human response in an efficient and cost-effective manner. However, lack of accurate *in vitro* predictions can result in a reluctance by the pharmaceutical industry to utilise such non-traditional formulation approaches. The past two decades have witnessed a surge in development of *in vitro* models for SEDDS including biorelevant dispersion, digestion and permeability testing, where increasingly detailed simulations of the GIT are seen (8-11). Additionally, prevalence of computational modelling, as well as *in silico* simulations based on physiology-based pharmacokinetic (PBPK) modelling platforms, such as Gastroplus, Simcyp and PK-Sim are steadily increasing (12, 13). While collaborative efforts are being made to improve *in vitro* and *in silico* tools (14, 15), the complexity of endogenous formulation processing results in gaps in development of accurate *in vivo* predictions. Resultantly, one method to increase prediction accuracy involves validation and optimisation of *in vitro* simulation conditions, via introduction of increasingly physiologically and biopharmaceutically relevant input parameters.

In addition, pre-clinical animal models provide invaluable early performance indicators for oral bioavailability, formulation performance and impact of dosing conditions (e.g. food effects) (13, 16-18). Usually this involves collection of plasma samples, but an additional opportunity exists for collation of animal gastrointestinal (GI) luminal aspirates and fluids for solubility screening (19).The utility of the pig model to reliably predict human *in vivo* behaviour has been previously reviewed (17), demonstrating high similarity with human GI conditions and physiology of commonly used breeds such as the domestic miniature-sized pig. However, while similar in anatomy and physiology, the chief principle of utilising animal models is their ability to provide a reliable estimate of *in vivo* performance of drug delivery systems in humans. It is, therefore, crucial that all biopharmaceutical processes are adequately simulated, including the ability of the intestinal fluids in the target species to provide a comparable solubilisation capacity to their human equivalents (3, 20). Resultantly, previous quantitative assessment of the composition of porcine GI fluids revealed differences in both the concentrations of solubilising components and in the relative quantities of the major bile acids when compared to human intestinal fluids (21). These observations led to the development of a porcine biorelevant medium, Fasted State Simulated Intestinal Fluid of pigs (FaSSIFp) based on the composition of porcine GI fluids with respect to pH, buffer capacity, osmolality, surface tension, as well as the bile salt, phospholipid and free fatty acid content in fasted state pigs (21). As these endogenous compounds and their interactions with LBF excipients have been suggested to be vital for solubilisation of PWSD in the GIT (19), further characterisation evaluating similarities and differences in the fluid ultrastructure's formed in both human and porcine fluids through microscopic evaluation is warranted. Furthermore, additional characterisation of fluid structures observed following SEDDS administration may provide insights regarding the capability of SEDDS to mimic post-prandial enhanced solubilisation and improve understanding of the mechanisms by which this enhanced solubilisation is generated.

In response to the necessity for validated *in vitro* models, this research sought to assess if a qualitative evaluation of porcine fluid ultrastructure, as discussed above, in combination with quantitative assessments of drug solubility in these fluids, could inform increasingly bio-predictive *in vitro* tools. In order to achieve this aim, morphological characteristics of porcine luminal media in the fasted and fed state, as well as at five time points post SEDDS ingestion were conducted at the ultrastructure level. While similar microscopic analysis of both human and simulated fluids have been conducted (5, 22), this research provides the first comparative analysis of porcine fluids using two complementary techniques of Cryogenic Transmission Electron Microscopy (Cryo-TEM) and Negative Stain TEM, previously demonstrated as excellent tools for such analyses (23). These qualitative observations were then compared to *ex vivo* solubility values to investigate any time dependent change in drug solubility post SEDDS ingestion. Fenofibrate was chosen as a BCS Class II neutral drug, and has previously displayed food effects in landrace pigs (18), where the lack of a pH effect between gastric and intestinal samples allowed direct comparisons. Using combined knowledge from the microscopic images and quantitative solubility studies, it was analysed if the maximum observed *ex vivo* solubility with SEDDS could be used to inform more physiologically relevant input parameters, supporting refinement of *in vitro* models for SEDDS.

2. Materials and methods

2.1. Materials

Fenofibrate was purchased from Kemprotec Ltd. (UK). Hard gelatine capsules (00EL Licaps®) were obtained from Capsugel®. All food components used in preparing the FDA recommended breakfast were purchased commercially. Fasted State Simulated Intestinal Fluid (FaSSIF) and Fasted State Simulated Gastric Fluids (FaSSGF) were produced from FaSSIF/FeSSIF/FaSSGF powder obtained from Biorelevant.com (Croyden, UK). For the fasted state simulated porcine media (FaSSIFp); Lipoid E PC S was obtained from Lipoid GmbH (Germany), Sodium taurodeoxycholate; Sodium hydroxide (NaOH) pellets; Chloroform; Sodium chloride (NaCl); Sodium dihydrogen phosphate monohydrate; Sodium oleate were purchased from Sigma Aldrich (Ireland) and sodium taurocholate was ordered from Thermo Scientific Ltd., Alfa Aesar (UK). Olive Oil, Tween 85 and Kolliphor RH 40 were all purchased from Sigma-Aldrich (Ireland). All other chemicals and solvents were of analytical grade or HPLC grade, respectively, and were purchased from Sigma–Aldrich (Ireland) and used as received. Water of HPLC grade was produced using a MilliQ system (Merck KGaA, Germany).

2.2. Gastric and intestinal fluid collection

This study was carried out under a licence issued by the Health Products Regulatory Authority (HPRA), Ireland and EU Statutory Instruments. Local University Ethical Committee approval was obtained. 11 male landrace pigs were sourced locally and housed individually at the Universities Biological Services Unit (17-20 kg and mean 18.3 kg). Pigs were fed approximately 175 g of standard weanling pig pellet feed twice daily and given free access to water. The final feed of 175 g was given 24 h prior to dosing. Pigs were grouped into either fasted state (3 pigs), fed state (3 pigs) or SEDDS group (5 pigs) for the *post mortem* assessment.

The following *post mortem* fluid collection protocol was repeated for the 3 groups. Firstly, the fasted state group (following a 24 hour fast) received 50 mL of water via a syringe 30 min prior to euthanasia and *post-mortem* sampling. The study was designed to mimic dosage conditions under a fasted leg of a pre-clinical study, therefore 50 mL of water was provided to mimic administration of a dose with water in pigs and access to water was thereafter restricted until sampling, in accordance with the standard protocol applied by Henze et al. (18). The fed state group of 3 pigs, were fed a half portion of a standard high-caloric, high-fat FDA breakfast, the mass which equated to approximately 18–20 g/kg of body weight. The fed group were given this FDA breakfast two hours prior to euthanasia and *post-mortem* luminal fluid sampling, where water was again restricted until sampling. The SEDDS group was orally administered with 1 g of a Type IIIa SEDDS via a dosing device in a gelatine capsule (00EL Licaps®, Capsugel®) followed by 50 mL of water via syringe. 1 g SEDDS was chosen to be representative of a commonly

administered amount in comparative animal studies using the landrace pig. SEDDS consisted of 40% Olive Oil (long chain triglyceride), 40% Tween 85 (co-surfactant) and 20% Kolliphor RH 40 (surfactant). Access to water was restricted up to 3 h post dosing. All pigs were euthanized humanely by intravenous injection of pentobarbital sodium followed by potassium chloride. The peritoneal cavity was exposed by midline incision and the stomach and small intestine were isolated. Occluding ligatures were applied proximal to the cardiac sphincter and distal to the pyloric sphincter as well as at the proximal and distal ends of the small intestine. Once both ends were secured, the stomach and small intestine were removed from the peritoneal cavity. The small intestine was sub-divided into three sections approximating to the duodenum (USI), jejunum (MSI) and ileum (LSI). Gastric, USI, MSI and LSI luminal fluids were then collected and transferred to sterile 50 mL sample tubes at time intervals of 0.5, 1, 2, 3 and 4 h post dosing respectively (n = 1). Further digestion in the samples post-sampling was inhibited with 1 μM orlistat (24). All samples were first immediately frozen at -20°C, then stored at -80°C until further analysis.

2.3. Cryogenic and negative stain transmission electron microscopy studies

All GI samples (fasted, fed and SEDDS) were centrifuged at 30,000 × *g* for 15 min at room temperature in an Optima MAX-XP Ultracentrifuge from Beckman Coulter (Brea, CA, USA) and the supernatant collected for ultrastructure characterisation. Cryo-TEM samples were prepared by depositing 3 μL of the supernatant (some diluted in ultrapure water to ensure proper vitrification) on glow-discharged 300 mesh lacey carbon grids from Ted Pella Inc. (Redding, CA, USA). Sample vitrification was then carried out in liquid ethane using a Vitrobot Mark IV from FEI (Hillsboro, OR, USA) under controlled (4 °C, 100% relative humidity) and automated conditions (blot time 3 s, blot force '0'). The vitrified samples were then kept in liquid nitrogen and images obtained with an accelerating voltage of 200 kV using a Tecnai G2 20 TWIN Transmission Electron Microscope equipped with a 4K CCD Eagle digital camera from FEI. Negative Stain TEM samples were prepared by depositing 4 μL on glow-discharged 200 mesh carbon grids from Ted Pella Inc. After 60 s, 10μL of water was added and the grids carefully aspirated using the edge of a filter paper. Gastric samples were then stained with 10μL of a uranyl acetate solution (pH 2) for 30s, while intestinal samples were stained with a phosphotungstic acid solution (pH 7). Lastly, the grids were washed twice with 10μL water and aspirated. Images were recorded using a CM100 TWIN Transmission Electron Microscope (Philips, Amsterdam, The Netherlands) with an accelerating voltage of 100 kV and equipped with a side-mounted Veleta Camera (Olympus). Use of both techniques allowed for cross-referencing of samples to verify presence of different colloidal structures and increased the robustness of the analysis.

2.4. Solubility studies

Ex vivo apparent solubility studies of fenofibrate were conducted on gastric and USI samples obtained from the SEDDS group at 0.5, 1, 2, 3 and 4 h post sampling, as well as fasted and fed gastric and USI samples. pH of the SEDDS samples was measured using a using a Model 3510 pH/mV/Temperature Meter (Jenway, UK). Fenofibrate was added in excess to triplicate glass vials containing a specified volume of each fluid pre-heated to 37°C and a magnetic stirrer. Vials were placed on a stirring plate at 300 rpm (Mixdrive 15, 2MAG, Germany) in a 37°C incubator for the period of the study. 150 μL samples were removed at 2, 4, 6 and 24 h, with the mean of the 24h samples used for data analysis. Samples were centrifuged at 11,400 × g for 10 min at 37°C (Mikro 200 R, Andreas Hettich GmbH & Co. KG, Germany), followed by a 10-fold dilution in acetonitrile. Next the samples were centrifuged a second time to remove precipitated proteins (11,400 × g, 10 min, 4°C). Supernatant was then transferred to a separate centrifuge tube and suitably diluted in mobile phase in preparation for analysis via RP-HPLC/UV.

In vitro solubility studies were carried out using commercial FaSSGF, FaSSIF along with FaSSIFp previously described (21). FaSSGF and FaSSIF were prepared using the Biorelevant.com protocol (Croyden, UK) and FaSSIFp was prepared using the previously published protocol (21). Fenofibrate solubility was obtained in FaSSGF, FaSSIF and FaSSIFp, as well as 1:50, 1:100, 1:200, 1:500 and 1:1000 i.e. 1 g:50 mL, 1 g:100 mL, 1 g:200 mL, 1 g:500 mL and 1 g:1000 mL, dilutions of SEDDS dispersed through mixing in the biorelevant medias (n = 3). The same method as above was followed, however, only one centrifugation at 37°C, 11,400 × g for 15 min was used. The solubility result for 1:200 dispersion of SEDDS in FaSSIF was obtained from a previous publication (25).

2.5. RP-HPLC/UV analysis

Detection of fenofibrate was conducted using an Agilent 1200 series HPLC system comprising a binary pump, degasser, autosampler and variable wavelength detector. Data analysis was conducted with EZChrom Elite version 3.2. A Waters Symmetry® C18 column (4.6 × 150 mm, 5 μm) maintained at 25°C was used during separation. The mobile phase used consisted of 80:20 (v/v) acetonitrile and sodium acetate 25 mM buffer adjusted to pH 5. The flow rate was 1 mL/min and the detection wavelength was 287 nm. The drug concentration in each vial was calculated from a calibration curve run on the same day. The solubility value presented was the mean value of the 24 h triplicate samples. The analysis displayed linearity over the range 0.01-25 μg/mL ($r^2 > 0.999$). The precision of the method at 1 and 10 μg/mL, expressed as the coefficient of variation, was 0.442% and 0.327% within days and 2.796% and 2.92% between days respectively.

2.6. Statistical analysis

Prior to statistical analysis, drug solubility data in the different *ex vivo* and *in vitro* media were compared to Levene's Test for Equality of Variances where a p-value <0.05 indicated a violation of equal variance. Solubility comparisons were conducted using a one-way ANOVA with pairwise comparisons of the groups completed using Tukey's multiple comparison test. All statistical analysis was conducted using SPSS (IBM, California) as p-value <0.05 indicated a significant result. Graphs of solubility and pH were obtained using Prism 5 (GraphPad Software, CA, USA).

2.7. In silico prediction

A multiple linear regression (MLR) equation previously developed to predict the solubility ratio (SR) of drugs upon SEDDS dispersion in FaSSIF relative to FaSSIF solubility (25) was employed. This equation was previously produced using Excel (Microsoft Office, 2016), where correlations were investigated between a selection of drug properties and SR for a database of 30 PWSD, resulting in Eq. 1:

$$logSR = 0.54 + 0.17(logD6.5) + 1.04(F\_AromB) - 0.01(T_m) \quad (1)$$

Where $logD_{6.5}$ is the partition coefficient at pH 6.5, F_AromB is aromatic bonds as a fraction of total bonds and T_m is the melting point of the drug (Fenofibrate). The antilog of the result was then multiplied by the solubility of fenofibrate in FaSSIF obtained from literature (26), in order to obtain the prediction of fenofibrate solubility upon SEDDS dispersion in FaSSIF and compared to the *ex vivo* and *in vitro* results obtained in this study.

3. Results

3.1. pH characterisation of gastric and intestinal porcine media with a SEDDS

In order to assess if administration of a SEDDS would alter the pH

profile in the GI fluids of pigs, post mortem samples of both the gastric and USI samples were collected at various time points post SEDDS administration in the fasted state. In total five pigs were administered a SEDDS formulation, and post mortem samples of the gastric and USI samples were collected at 0.5,1,2,3 and 4 hours (n = 1) (Fig. 1). Due to the limited sample availability, no pH could be obtained for USI at 0.5 h. In terms of the gastric samples, after 30 min the low pH value observed was in line with previously reported values of fasted state pH in landrace pigs (range reported 1.2 - 4.0) (17). However, at 1 h the pH observed was higher (5.37), while values appeared to subsequently fall back to low levels thereafter. However, given that only one sample was available, limited statistical relevance can be derived. The pH of the USI samples ranged from 5.06 - 7.67, consistent with previous fasted-state observations in the landrace pig (17). Overall, it would appear that administration of SEDDS has a limited effect overall on gastric and USI pH over the 4 hour period, and while further studies would be required in a larger number pigs, to assess a transient increase in gastric pH, such studies were not considered justified given the findings of this initial pilot study.

3.2. Microscopic evaluation of fasted and fed state gastric and intestinal porcine fluids

Two complementary techniques of Cryo-TEM and Negative Stain TEM were used (Fig. 2). For the fasted-state, Cryo-TEM and Negative Stain gastric images revealed the presence of small structures, which may represent micelles and a vesicle/lipid droplet (~100-150 nm). In the USI fasted state samples, bilamellar vesicles (200 nm), a ruptured vesicle (~400 nm) and small micelle-like structures (10-30 nm) were the predominant features. A MSI fasted sample also revealed an abundance of fiber-like structures. In the fed-state gastric images, while micelles (10-50 nm) were seen, overall these images displayed evidence of a heterogeneous population with clustering of structures and higher concentrations of colloidal structures of different sizes ranging from approximately 50-500 nm. Structures observed included unilamellar vesicles, multi-compartmental vesicles and multilamellar vesicles and lipid droplets. In terms of the USI images, once again clusters of multivesicular structures including unilamellar, bilamellar and multi-compartmental vesicles were dominant (approximately 100-600 nm). Furthermore, either a mixed micelle or lipid droplet was seen (100 nm), as well as a mixture of micelles and vesicles in the Negative Stain TEM USI and MSI samples.

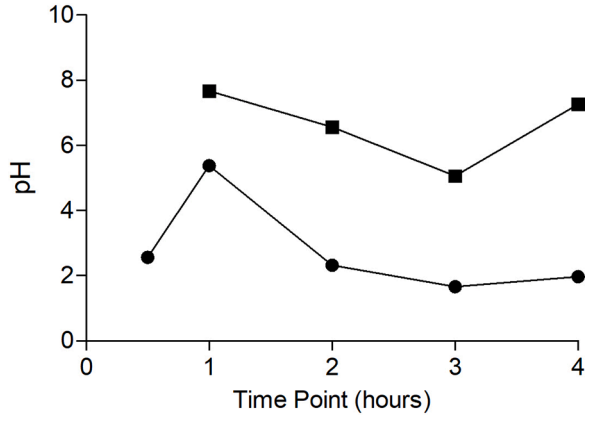

Fig. 1. pH values obtained as a function of time from gastric (black circles) and USI samples (black squares) following administration of a placebo SEDDS to fasted pigs (n=1).

3.3. Microscopic evaluation of porcine gastric and intestinal fluids post administration of a placebo SEDDS

Changes in luminal fluid ultrastructure were observed at different time points (0.5, 1, 2, 3, 4 h) post SEDDS oral administration in the fasted state. Cryo-TEM images were obtained for the 0.5, 1 and 2 h SEDDS samples only (due to sample unsuitability) and Negative Stain TEM images for each sampling point, except 0.5 h USI and MSI and 3 h MSI (no sample collection) (Figs. 3 and 4). When compared to the fasted state gastric composition, high concentrations of small micelles 10-40 nm are seen in the 0.5, 1 and 2 h Cryo-TEM images, in addition to small lipid structures (20-60 nm) after SEDDS administration. In terms of the USI Cryo-TEM images, the 1 h samples demonstrated examples of what resembled lipid droplet clusters, similar in appearance to structures seen in the 2 h gastric and fed state USI samples (Fig. 3). SEDDS administration did not appear to produce similar multivesicular structures to the fed state, while a clear difference in composition was observed from the fasted state in terms of higher concentrations of micelles and clusters of lipids droplets, particularly at the 1 h sampling point.

Similarly, Negative Stain TEM revealed differences between SEDDS administration and the fasted and fed state (Fig. 4). Firstly, similar to Cryo-TEM a high concentration of small lipid structures 10-40 nm were visualised in the 0.5 h gastric image. The 1 h gastric image revealed a heterogeneous mix of structures with a higher concentration of structures versus the fasted state. A large lipid droplet or vesicle, approximately 200-250 nm in diameter, could be observed and was similar in appearance to structures observed in the fed state gastric sample. In the 2 h gastric, USI and MSI samples, vesicles/lipid droplets (100-200 nm) were observed, while the compositional characteristics of the 3 h samples depicted a great mix of micelles and vesicles of 10-200 nm. Interestingly, the 4 h samples, appeared similar in overall composition to the previous fasted state images, in terms of appearance of small structures resembling micelles (10-50 nm), and fiber-like structures.

3.4. Fenofibrate solubility in pig gastric and intestinal media post ingestion of a placebo SEDDS

To investigate potential correlations with the colloidal species visualised upon microscopic evaluation of the SEDDS samples, *ex vivo* solubility studies using gastric and USI fluids were conducted. These results were also compared to the *ex vivo* fed, fasted and biorelevant media solubility results (Fig. 5). As seen in Fig. 5, in both the gastric and USI samples, the highest *ex vivo* solubility was observed 1 h post SEDDS ingestion where both samples displayed similar values, while the lowest solubility was at 4 h. In terms of gastric solubility at each time point, fenofibrate solubility increased from 0.5 h (189 ± 10 μg/mL) to 1 h (285 ± 31 μg/mL) post ingestion (Fig. 5). After the 1 h sample, a decrease in drug solubility was seen, where 2 h (61 ± 8 μg/mL) and 3 h (68 ± 4 μg/mL) samples displayed similar solubility, both below the value obtained from the gastric fed state sample (86 ± 6 μg/mL). Finally, the 4 h sample displayed a low drug solubility (9 ± 4 μg/mL), similar to the value obtained from fasted gastric media (6 ± 2 μg/mL). USI samples displayed a similar solubility trend, though no sample fluid could be collected for the 0.5 h sample thus, was not available for comparisons. Once again, the 1 h time point demonstrated the highest drug solubility (271 ± 36 μg/mL). After this time, drug solubility decreased substantially as solubility at 2 h (117 ± 12 μg/mL) was higher than the 3 h (85 ± 9 μg/mL) sample in contrast to the gastric samples where 2 h and 3 h displayed similar values. In this case, the 2 h sample did exceed the fed state USI solubility obtained (104 ± 19 μg/mL), however not significantly ($p > 0.05$). Again, the lowest drug solubility was observed at 4 h (4 ± 1 μg/mL), also similar to the fasted state USI sample (7 ± 1 μg/mL).

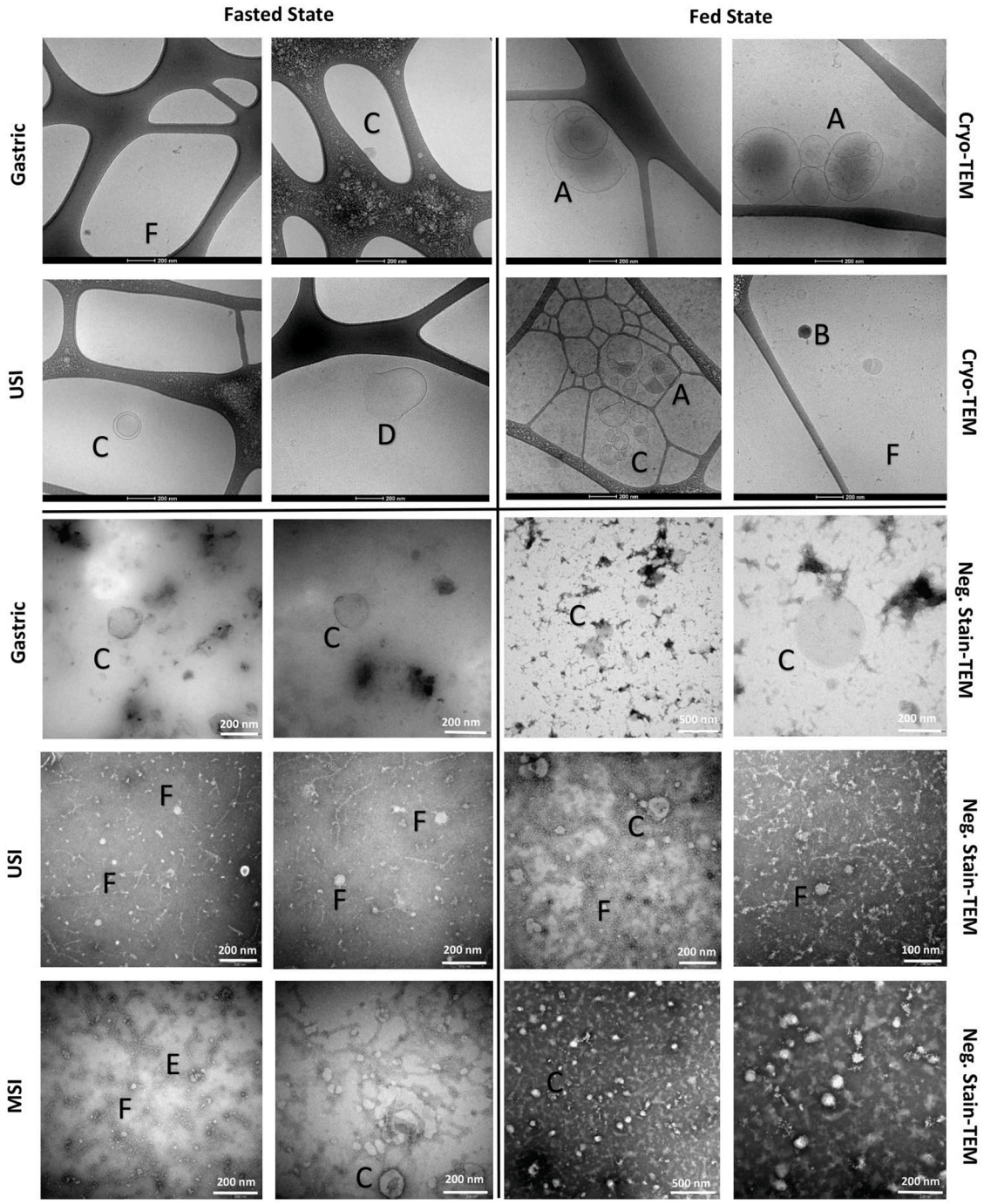

Fig. 2. Cryo-TEM and Negative Stain TEM images of fasted and fed state (2 h post-prandial) Gastric and Intestinal samples. Letters indicate representative colloidal structures. A (Multi-Compartmental Vesicles 200-800 nm), B (Lipid droplet), C (Unilamellar and Bilamellar Vesicles or Lipid Droplets 150-400 nm), D (Ruptured Vesicle 400 nm), E (Fiber-like structures), F (Micelles/Small structures 10-50 nm). Measurement scales are shown. To ensure proper vitrification the fed state USI samples were diluted in ultrapure water.

3.5. Exploration of in vitro SEDDS screening tool using enhanced biorelevant media and investigation of appropriate dilution conditions

Apparent solubility was determined in SEDDS dispersions in simulated human or simulated porcine fluids and compared to the apparent solubility from the *ex vivo* studies where 1 g of SEDDS was administered. The gastric and intestinal *ex vivo* 1 h samples were taken as an approximation of the maximum *in vivo* solubility with SEDDS, and consequently, as the value which the *in vitro* conditions should replicate. Apparent solubility was determined in 1:50, 1:100, 1:200, 1:500 or 1:1000 dispersions of SEDDS in the various biorelevant medias (FaSSGF, FaSSIF, FaSSIFp). All medias containing dispersed SEDDS were significantly different from the solubility of fenofibrate in the respective medias alone ie. FaSSGF (0.25 ± 0.01 μg/mL), FaSSIF (9.6 ± 1.4 μg/mL) and FaSSIFp (15.69 ± 0.9 μg/mL). One-way ANOVA analysis and a Tukey post-test found that in the three medias, no significant difference was found between the *ex vivo* results and *in vitro* solubility in the 1:200 SEDDS media (Fig. 6). Conversely, in all three media, the 1:50, 1:100, 1:500 and 1:1000 dispersions significantly differed ($p < 0.05$) from the *ex vivo* 1 h gastric and 1 h USI results respectively. The 1 h USI *ex vivo*

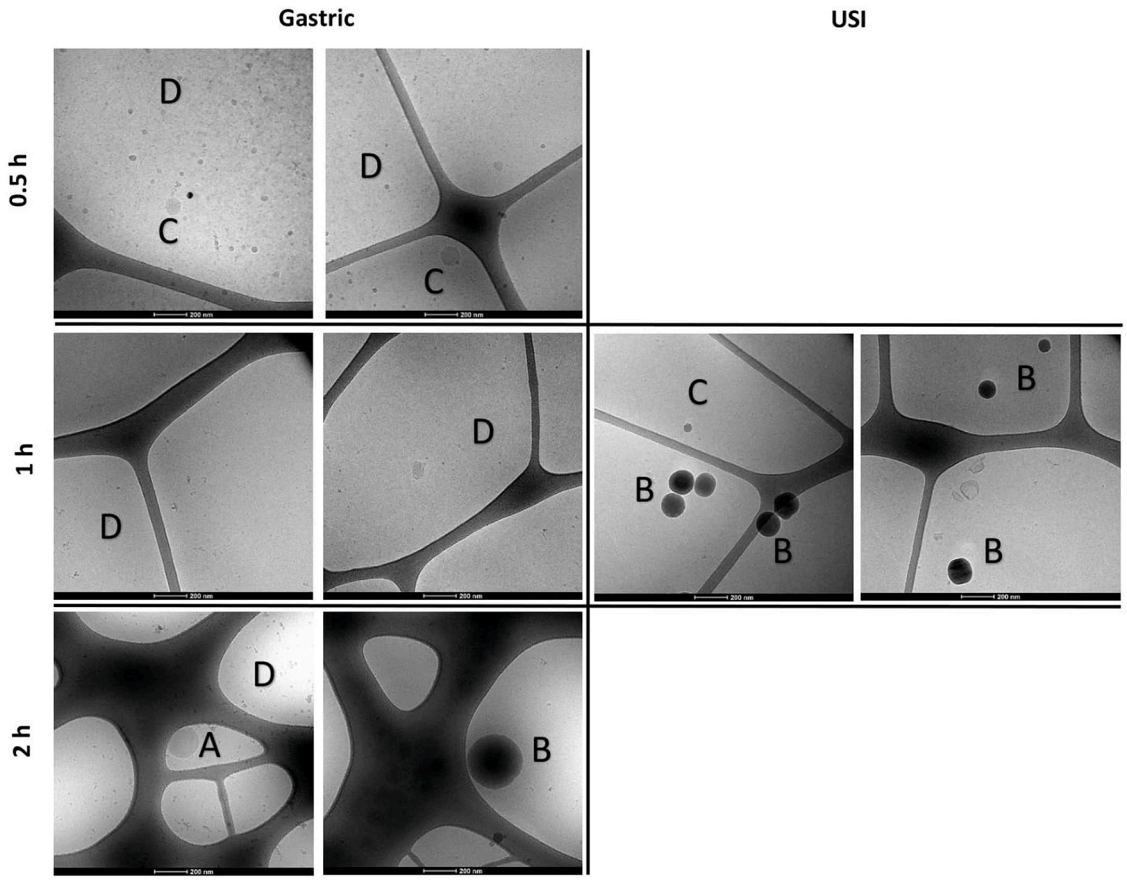

Fig. 3. Cryo-TEM images of SEDDS Gastric and USI fluids at 0.5, 1 and 2 h post SEDDS administration. Letters indicate representative colloidal structures. A (Unilamellar Vesicles 100-600 nm), B (Lipid Droplet), C (Small Lipid Structures 20-60 nm), D (Small Micelles 10-40 nm). A 200 nm scale is shown for all images. To aid proper vitrification the 1h USI samples were diluted in ultrapure water.

solubility and 1:200 *in vitro* solubility results in FaSSIF were also not significantly different from the solubility predicted from a previously published equation which predicts drug solubility gain upon SEDDS dispersion (25).

4. Discussion

The increasing demand for bio-enabling drug delivery systems has generated a complementary necessity for predictive tools to support data-driven, model-informed formulation development. Ability to confidently discriminate formulation performance using *in vitro* tools is key for successful implementation of modern enabling drug delivery approaches. While combined pressures of traditional production familiarity, cost effectiveness and time constraints reinforce the importance of both accurate and efficient tools to encourage adoption of novel bio-enabling technologies. In recent decades, research has focused on standardization and increasing the physiological relevance of such tools (27). However, significant gaps in understanding limit ability to consistently predict *in vivo* drug luminal behaviour. Accordingly, the OrBiTo (Oral Biopharmaceutics Tools) project collaborators have highlighted importance of validation of *in vitro* and *in silico* models, through identifying key *in vivo* processes to be simulated and optimizing experimental inputs to reflect the identified variables (14, 27). Consequently, this research aimed to establish if, through microscopic and quantitative assessment of porcine fluids, *in vitro* simulation conditions could be improved through increasingly physiologically relevant input parameters. It is hoped that such a refinement of *in vitro* conditions can support the developability of drugs with SEDDS, through the facilitation of increasingly accurate *in vitro* dose number predictions.

The first step in achieving this aim involved obtaining an improved understanding of the landrace pig model, via a microscopic characterisation of pig luminal fluid ultrastructure. Aiming to reinforce the utility of the landrace pig model, while also aiding creation of increasingly bio-reflective *in vitro* conditions. Morphological characterisations on gastric, USI and MSI fluids were conducted using two microscopic techniques; Cryo-TEM and Negative Stain TEM. Firstly, fasted and fed state ultrastructures were microscopically compared and contrasted. Distinct morphological differences were observed between the fasted and fed state samples due to increased prevalence of clustering and generally larger structures in the latter. The exact composition of the fasted gastric samples were more difficult to elucidate due to the lack of comparative studies investigating human gastric fluids, perhaps suggesting scope for future research. For example, the somewhat unexpected presence of small micelle resembling structures in both the fasted and 4 h SEDDS gastric samples, is in line previous reports of high bile salt concentrations in the landrace pig stomach compared to humans (21). Most likely reflecting reflux of bile from the pig duodenum to the stomach. In terms of intestinal samples, the fasted intestinal fluids did suggest, in addition to fiber-like structures and vesicles, evidence of spherical micelles, previously shown to be abundant in FaSSIF and Fasted State Human Intestinal Fluids (FaHIF) (5, 22, 23). Similar vesicular components of approximately 100 nm have also been found in FaSSIF (5, 28).

In contrast, the more complex composition of the fed state samples displayed evidence of clustering and larger multivesicular structures. The heterogeneous fed state presentation was expected as previous research demonstrated large variability in fed state human intestinal fluids (FeHIF) compared to FaHIF ultrastructure (23). The irregular appearance of some larger structures (>200 nm) has previously been

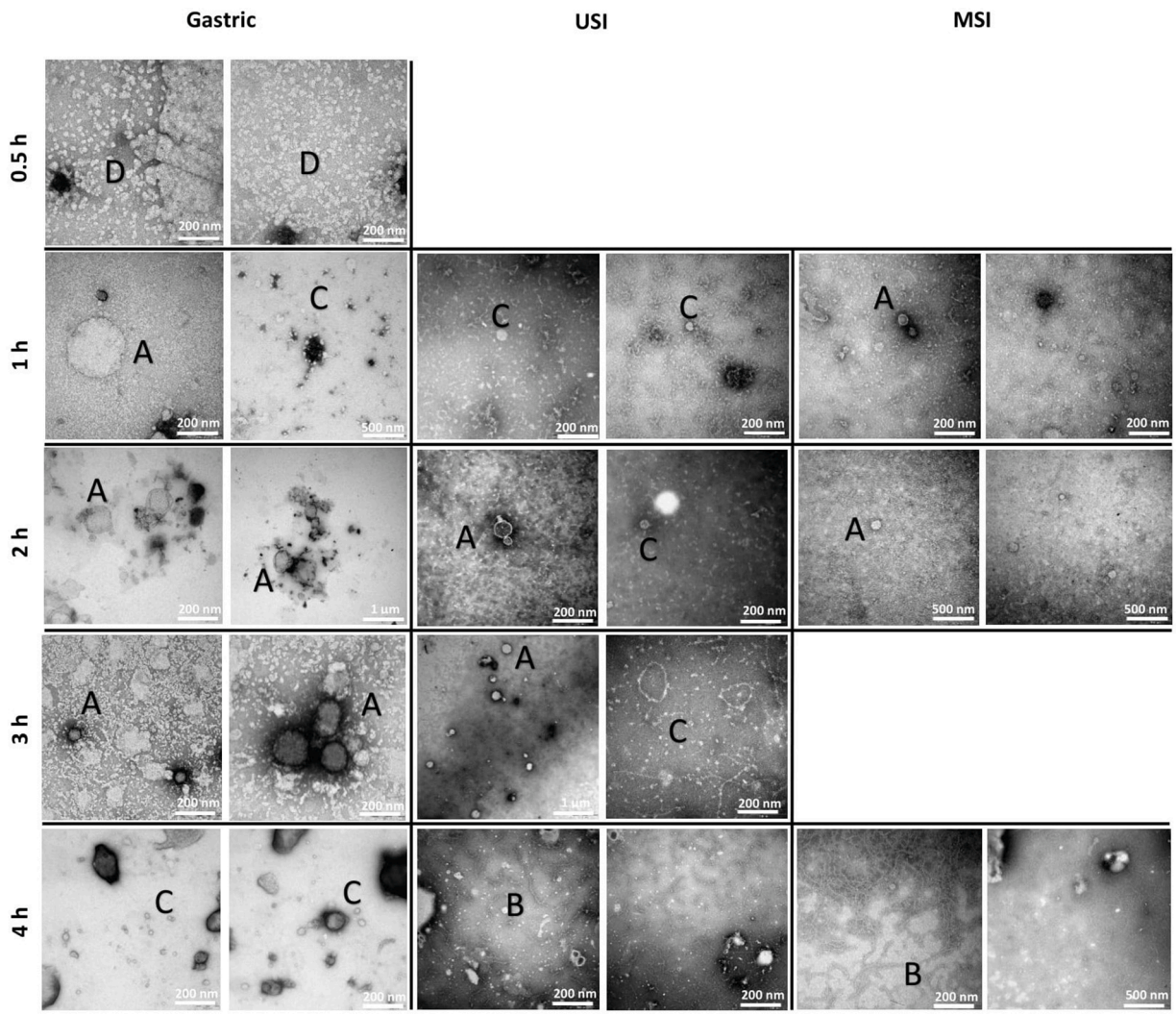

Fig. 4. Negative Stain TEM images of SEDDS gastric and intestinal fluids at 0.5, 1, 2, 3 and 4 h post placebo SEDDS administration. Letters indicate representative colloidal structures. A (Vesicles 200-400 nm), B (Fiber-like Structures), C (Micelles/Small Structures 10-60 nm), D (Small Lipid Structures 10-40 nm). Measurement scales are shown for each image.

related to their dynamic transient nature as intermediate phases (29, 30). The fed state images in this study resembled the ultrastructure of FeSSIF including micelles and structures ranging from unilamellar to multicompartmental vesicles (23). This is reflective of previous observations that while uni-, bi- and multilamellar vesicles dominate in FeHIF they are rarely seen in FaHIF (22). However, upon comparison of the porcine fed state intestinal fluid to fed state human intestinal fluids, the structures observed appeared generally smaller in these porcine samples, as numerous elongated structures from 1-10 µm have been observed in FeHIF (23, 29, 31). While similar structures would be expected in general, significant differences in ultrastructure between pigs and humans is likely related to differences in rates of digestion, major primary bile acids (17), total phospholipid and cholesterol concentrations along with differences in bile salt: phospholipid ratios (21). When compared to previous work demonstrating capacity for landrace pigs to predict food effects (18), from these images, it is clear that such an effect is produced through large clusters of heterogeneous vesicular structures in the fed state compared to the fasted state, capable of increasing the solubility of PWSD. Accordingly, an impact of this work is that porcine GI fluid ultrastructure, while demonstrating differences to human and simulated fluids, also shares common characteristics of these fluids, aiding its simulation of human luminal fluids.

Microscopic analysis was additionally conducted to investigate how porcine luminal fluids responded to SEDDS administration. Similar to the food effect, understanding of the *in vivo* SEDDS solubilisation process is a key consideration for the development of predictive tools. SEDDS performance is often related to a bridging of the fasted-fed solubility gap, therefore, it was investigated if SEDDS administration led to production of colloidal species more closely resembling the fed state. Images of gastric and intestinal media samples taken periodically up to four hours post placebo SEDDS administration revealed time dependent SEDDS processing *in vivo* through differences in colloidal and lipid structures. Compared to fasted gastric samples, high concentrations of small micelles ranging from 20-40 nm and larger lipid structures were seen in the 0.5 h gastric SEDDS sample, resembling higher concentrations of small micelles previously seen in fed state simulated intestinal fluids (FeSSIF) and FeHIF (5, 23). The 1 h SEDDS USI samples displayed a large unilamellar vesicle and clusters of lipid droplets, similar to the USI fed sample, previously observed in FeSSIF, FeSSIF-V2 and FeHIF (23, 31). While a similar lipid droplet was seen in the 2 h gastric sample. From these images it appears that the SEDDS droplets formed ranged from 100-200 nm approximately. This can be compared to smaller previous size estimates of 44.76 ± 0.303 nm and 51.7 ± 0.8 nm observed for this SEDDS dispersed in FaSSIF and simulated gastric fluid without pepsin (SGFsp) respectively (25, 32). However, effect of digestion on droplet size was not accounted for in these previous studies. This along

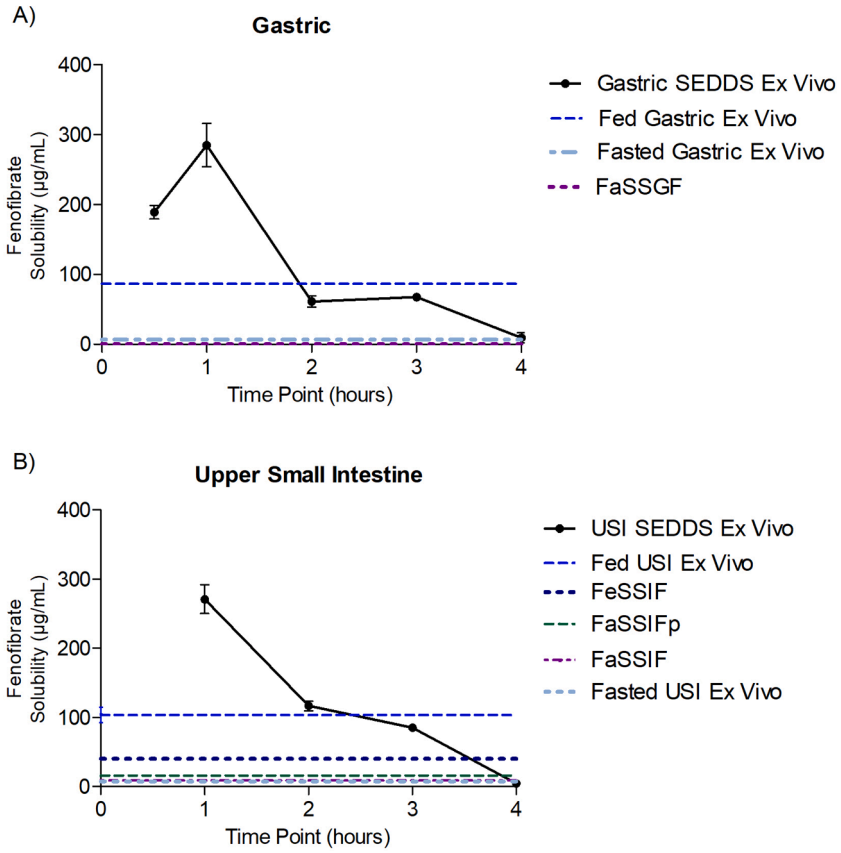

Fig. 5. A) Fenofibrate solubility in gastric porcine luminal fluids 0.5, 1, 2, 3 and 4 h post placebo SEDDS ingestion for five pigs (Gastric SEDDS Ex Vivo) compared to fasted and fed gastric porcine (2 h post-prandial) and FaSSGF apparent solubility (n = 3). B) Fenofibrate solubility in USI porcine luminal fluids 1, 2, 3 and 4 h post placebo SEDDS ingestion for four pigs (USI SEDDS Ex Vivo) compared to fasted and fed USI, FaSSIF, FeSSIF and FaSSIFp solubility (n = 3).

with differences in bile salt and phospholipid constituents and concentrations between the *in vivo* porcine and human simulated media, likely explains the smaller sizes seen.

From these images it appears that SEDDS administration does not result in colloidal structures of the same complexity and size of fed state fluids, with the differences in types and concentrations of lipids present, along with the added complexity of the surfactant present in the SEDDS samples playing a role. In contrast, clusters of lipid droplets from SEDDS processing were seen, predominantly in numerous 1 h USI samples. This can be compared to previous work where small micelles and clusters of lipid droplets were microscopically observed at the beginning of lipolysis during *in vitro* SEDDS digestion and fewer lipid droplets were seen as time progressed, suggesting complete digestion (33). Clear differences between the 0.5 h to 4 h SEDDS samples were seen. When compared to the fasted state Negative Stain TEM images, similarities were perceived with the 4 h SEDDS images in terms of the predominant presence of fiber-like structures and small structures resembling micelles. Overall, this microscopic assessment suggests that the colloidal structures formed post SEDDS ingestion, while demonstrating increased colloid numbers relative to the fasted state, appear less complex than fed state fluids. While other physiological effects such as transit times may also play a role in differences seen in the media.

Following the observation of varied colloidal structures in the gastric and intestinal fluids, and presence of lipid droplet clusters in the 1 h USI sample during microscopic analysis, it was then assessed if these qualitative observations could be correlated to time dependent changes in fenofibrate solubility from 0.5 h up to 4 h post SEDDS administration. Accordingly, the differing drug solubility's seen at the various time points can be related to time dependant digestion of the vehicle and potential on-going lipid absorption. Solubility in both the gastric and USI samples was highest at 1 h post administration, exceeding fed state solubility, before decreasing at 4 h to levels similar to fasted state gastric and USI fluid and simulated fasted media. Resultantly, for fenofibrate, which displays a high solubility in this SEDDS (96.6 ± 3.4 mg/mL) (32). It appears to be the presence of the SEDDS lipid droplets, as seen in the 1 h USI images, which are likely to be the key reservoirs of drug, maintaining high solubilisation capacity.

In summation, the images 1 h after SEDDS administration, the time of maximum observed *ex vivo* drug solubility, appeared different in colloidal ultrastructure composition, compared to the fasted state fluid, and also the fed state fluids 2 h after feeding. In the fed state, the lipid load produced is likely higher and more diverse, reflecting the complexity of the meal composition, likely contributing to differences observed with the SEDDS samples. While it appears from this study that the increased fenofibrate solubilisation using SEDDS is primarily driven through presence of SEDDS lipid droplets. It must be acknowledged that a different SEDDS may produce a different outcome in such a study and these results represent a snapshot reflecting the ingested type and amount of SEDDS ingested. Any solubilising effect of the SEDDS was lost at 4 h, where fenofibrate solubility mirrored fasted state gastric and USI values. In agreement, the Cryo-TEM 4 h images resembled the fasted state, with these results both suggesting that by this time the GIT had sufficiently processed the SEDDS, and digestion and absorption was complete. A contributing factor may also be that from 3 h after SEDDS administration pigs received *ad libitum* water access, potentially accelerating flushing of the SEDDS at 4 h.

Previous research has investigated the drug solubilisation effect of carvedilol in canine intestinal fluids, where administration of 2 g of LBF resulted in a significantly higher solubility in fluids collected 5-20 min after administration versus 1 g of LBF or water (34). This higher

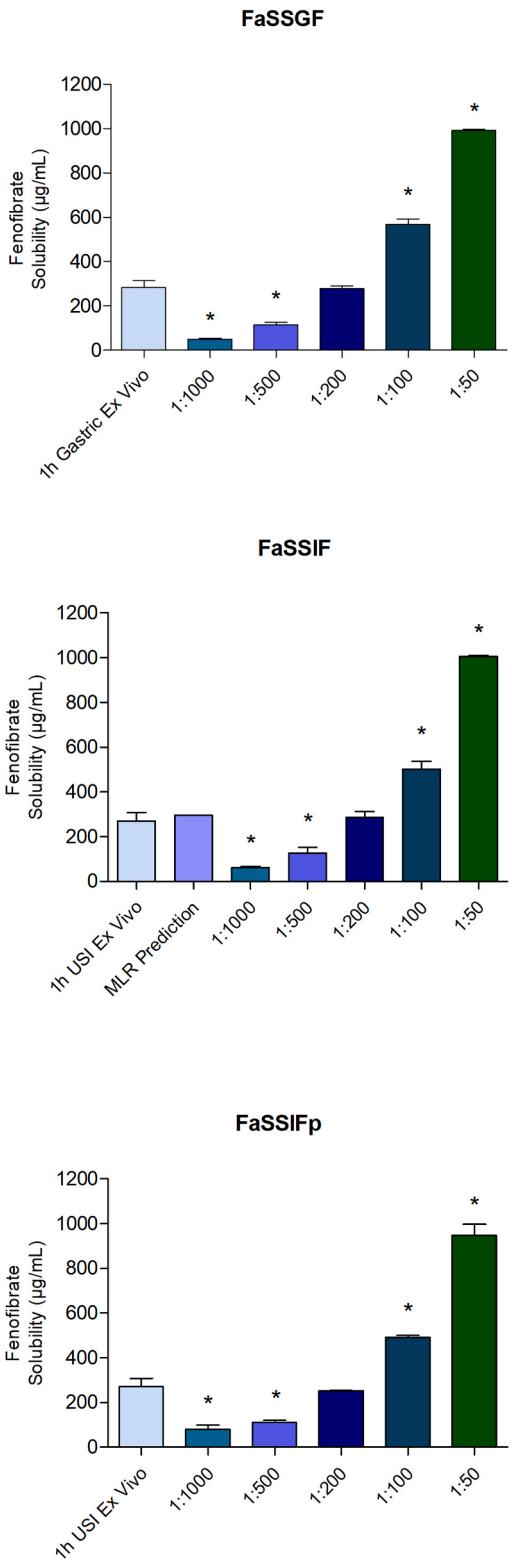

Fig. 6. Maximum fenofibrate *ex vivo* solubility in Gastric and USI luminal fluid 1 h after SEDDS administration compared to FaSSGF, FaSSIF and FaSSIFp media supplemented with 1:50, 1:100, 1:200, 1:500, 1:1000 dispersions of SEDDS. A one-way ANOVA and Tukey post-test revealed no significant difference between solubility in the porcine fluids versus the three biorelevant media with a 1:200 dilution. A predicted solubility upon SEDDS dispersion in FaSSIF from MLR also displayed no significant difference from the *ex vivo* USI result. * represents a significant difference ($p < 0.05$) of mean solubility compared the *ex vivo* solubility measurement in each graph i.e. 1 h Gastric Ex Vivo or 1 h USI Ex Vivo.

solubility was only seen for the 5-20 min samples, and not samples taken at 0-5 min or 20-90 min after LBF administration. Differences in the timeframe of maximum observed solubility between these two studies is likely as a result of the previously discussed differences in absorption rates between canines versus pigs. Where the rate of drug absorption and gastric emptying in pigs is suggested to be marginally slower than canines (17). Meanwhile, in this study, solubility in fasted and fed state *ex vivo* USI samples, 7 ± 1 and 104 ± 19 µg/mL, respectively, appeared similar to reported human values for fenofibrate solubility in FaHIF (20 ± 26 µg/mL) and FeHIF (148 ± 60 µg/mL) (26). Overall, these results reflect the fact that while inter-species differences are inevitable and some weaknesses may exist for use of the porcine model, merits for its ability to provide close predictions of human solubility are clear.

Stemming from the combination of qualitative and quantitative assessments of porcine fluids post SEDDS ingestion, solubility at 1 h post SEDDS ingestion appeared highest for both gastric and USI fluids. Therefore, it appears that in order to accurately represent the maximum solubility estimate for dose number solubility classification, as outlined in the Developability Classification System (DCS), use of this 1 h media would provide the best solubility approximation when a SEDDS approach is considered. Accordingly, using knowledge obtained from the porcine fluid assessments in this study, *in vitro* testing was conducted to assess if this solubility estimate could be closely replicated *in vitro* using supplemented biorelevant media under optimal screening conditions. While use of *in vitro* models provide welcomed resources to predict *in vivo* formulation performance, they remain only as accurate as the precision of the experimental parameters upon which they are based. Even though appropriate simulation of *in vivo* relevant fluid volumes has been suggested to be critical for correct implementation of biopredictive tools (35), typically, testing parameters utilised, including dilutions, are taken from previous research and repeated, which may not represent an accurate bio-simulation of the conditions being replicated. Resultantly, it was hypothesised that a refined biorelevant medium reflecting the highest solubility observed from the microscopic and quantitative assessments in this study, could provide a more predictive and physiologically relevant estimation of how the GIT responds to SEDDS ingestion. In order to investigate which *in vitro* dispersion conditions provided the closest estimate of the 1 h *ex vivo* result, five different ratios of SEDDS dispersed (1:50, 1:100, 1:200, 1:500 and 1:1000) in three different biorelevant media were tested. These dispersions were selected as being reflective of the current physiological volumes suggested for the human small intestine, which vary from approximately 50-1100 mL (36, 37), while approximation is complicated through complementary presence of absorption. While the testing dilutions also approximated the 250 mL BCS solubilisation parameter (38) and 500 mL Developability Classification System (DCS) dose number solubilisation parameter (39), they also considered dilutions typically used for *in vitro* dynamic dispersion testing using dissolution testing apparatus (USP 2) (10, 32). As such, this also aimed to provide justification for traditional dispersion practises used in current *in vitro* tools to reflect the maximum solubilisation effect of 1 g of SEDDS administered in an *in vivo* study, a typical desired dose for humans.

Accordingly, this work succeeded in verifying that a 1:200 dispersion of SEDDS in biorelevant media provides the closest simulation of maximum *ex vivo* solubility after 1 h upon administration of 1 g of SEDDS. SEDDS dispersed 1:200 in all three media (FaSSGF, FaSSIF and FaSSIFp) displayed no statistically significant differences from the *ex vivo* 1 h SEDDS solubility value in gastric and USI porcine fluids (Fig. 6). Suggesting that biorelevant media containing 1:200 dispersed SEDDS should be used to accurately reflect likely maximum solubility *in vivo* after 1 h when 1 g of SEDDS is administered. Furthermore, as no statistically significant differences were found between solubility in the (1:200) FaSSGF, FaSSIF, FaSSIFp, or the *ex vivo* 1 h SEDDS gastric and USI samples, the earlier hypothesis, from the microscopy and solubility assessments, regarding the importance of the SEDDS droplets for solubilisation was reinforced. As these similar solubility values suggest that

the SEDDS excipients are primarily driving fenofibrate solubility in the SEDDS dispersions in contrast to any altered concentrations of bile salts and phospholipids or products of digestion in the respective medias. Additionally, accuracy of a previously published *in silico* tool for predicting solubility gain and resultantly dose number and DCS classification upon SEDDS dispersion in biorelevant media was verified when the predicted value (297 μg/mL) was similar to the *ex vivo* (1 h USI) and *in vitro* (1:200) solubility estimates (Fig. 6). Therefore, accurate prediction of the *in vivo* and *in vitro* measurements through this *in silico* modelling reinforces its applicability to reliably predict dose numbers with SEDDS. Overall, an improved *in vitro* screening tool using appropriately concentrated SEDDS dispersions accurately predicted maximum *in vivo* drug solubility, demonstrating the significance of *in vitro* tool validation.

5. Conclusion

Overall, implications of this work for wider research are numerous. The ability of microscopic and solubility analysis of porcine fluids to refine *in vitro* predictions with SEDDS was realised upon demonstration that solubility at 1 h post SEDDS administration was closely matched by a 1:200 dispersion of SEDDS in various biorelevant media. Resultantly, this study demonstrates that tailoring of formulation screening with refined bio-relevant inputs is of the utmost importance. While there will always remain a need for certain *in vivo* studies, characterisation of these systems can lessen dependence and aid progression to a more confirmatory, rather than exploratory role, via improvements in the predictive power of *in vitro* tools. Furthermore, this study represents the first characterisation of GI colloidal phases in pigs using advanced microscopic techniques, forming the basis for a better understanding of the landrace pig as a model for evaluating drug bioavailability from SEDDS, while providing increasing evidence for its close representation of human solubilisation capacity. Overall, through integration of qualitative and quantitative *ex vivo* porcine GI fluid characterisations and solubility estimates with *in vitro* tools, this work has demonstrated that refined predictions of *in vivo* drug solubility are achievable.

Credit author statement

Harriet Bennett-Lenane: Writing- Original draft, Methodology, Conceptualization

Jacob R. Jørgensen: Microscopic Analysis and Methodology

Laura J. Henze, Niklas J. Koehl: Data Curation

Joseph P. O'Shea, Anette Müllertz, Brendan T. Griffin: Supervision

Acknowledgements

We acknowledge the Core Facility for Integrated Microscopy, Faculty of Health and Medical Sciences, University of Copenhagen. This work was supported under funding from the Irish Research Council Post Graduate Scholarship Project number GOIPG/2018/883. Niklas J. Koehl, Laura J. Henze are part of the PEARRL European Training network, which has received funding from the Horizon 2020 Marie Sklodowska-Curie Innovative Training Networks programme under grant agreement No. 674909. The idea for this work resulted from a workshop attended as part of the UNGAP COST ACTION CA16205 funded by the Horizon 2020 Framework Programme of the European Union.

References

1 Bergström, CAS, Porter, CJH., 2016. Understanding the Challenge of Beyond-Rule-of-5 Compounds. Adv. Drug Deliv. Rev. 101, 1–5. https://doi.org/10.1016/j.addr.2016.05.016.

2 Bergstrom, CAS, Charman, WN, Porter, CJH., 2016. Computational prediction of formulation strategies for beyond-rule-of-5 compounds. Adv. Drug Deliv. Rev. 101, 6–21. https://doi.org/10.1016/j.addr.2016.02.005.

3 Clarysse, S, Brouwers, J, Tack, J, Annaert, P, Augustijns, P., 2011. Intestinal drug solubility estimation based on simulated intestinal fluids: comparison with solubility in human intestinal fluids. Eur. J. Pharm. Sci. 43 (4), 260–269. https://doi.org/10.1016/j.ejps.2011.04.016.

4 Bennett-Lenane, H, O'Shea, JP, O'Driscoll, CM, Griffin, BT, 2020. A Retrospective Biopharmaceutical Analysis of >800 Approved Oral Drug Products: Are Drug Properties of Solid Dispersions and Lipid-Based Formulations Distinctive? J. Pharm. Sci. 109 (11), 3248–3261. https://doi.org/10.1016/j.xphs.2020.08.008.

5 Clulow, AJ, Parrow, A, Hawley, A, Khan, J, Pham, AC, Larsson, P, et al., 2017. Characterization of Solubilizing Nanoaggregates Present in Different Versions of Simulated Intestinal Fluid. J. Phys. Chem. B 121 (48), 10869–10881. https://doi.org/10.1021/acs.jpcb.7b08622.

6 Christiansen, ML, Holm, R, Abrahamsson, B, Jacobsen, J, Kristensen, J, Andersen, JR, et al., 2016. Effect of food intake and co-administration of placebo self-nanoemulsifying drug delivery systems on the absorption of cinnarizine in healthy human volunteers. Eur. J. Pharm. Sci. 84, 77–82. 10.1016/j.ejps.2016.01.011.

7 Perlman, ME, Murdande, SB, Gumkowski, MJ, Shah, TS, Rodricks, CM, Thornton-Manning, J, et al., 2008. Development of a self-emulsifying formulation that reduces the food effect for torcetrapib. Int. J. Pharm. 351 (1–2), 15–22. https://doi.org/10.1016/j.ijpharm.2007.09.015.

8 Fagerberg, JH, Tsinman, O, Sun, N, Tsinman, K, Avdeef, A, Bergstrom, CA., 2010. Dissolution rate and apparent solubility of poorly soluble drugs in biorelevant dissolution media. Mol. Pharm. 7 (5), 1419–1430. https://doi.org/10.1021/mp100049m.

9 Keemink, J, Mårtensson, E, Bergström, CAS., 2019. Lipolysis-Permeation Setup for Simultaneous Study of Digestion and Absorption in Vitro. Mol. Pharm. 16 (3), 921–930. https://doi.org/10.1021/acs.molpharmaceut.8b00811.

10 Berthelsen, R, Klitgaard, M, Rades, T, Müllertz, A., 2019. In vitro digestion models to evaluate lipid based drug delivery systems; present status and current trends. Adv. Drug Deliv. Rev. 142, 35–49. https://doi.org/10.1016/j.addr.2019.06.010.

11 O'Dwyer, PJ, Box, KJ, Koehl, NJ, Bennett-Lenane, H, Reppas, C, Holm, R, et al., 2020. Novel Biphasic Lipolysis Method To Predict in Vivo Performance of Lipid-Based Formulations. Mol. Pharm. 17 (9), 3342–3352. https://doi.org/10.1021/acs.molpharmaceut.0c00427.

12 Persson, LC, Porter, CJ, Charman, WN, Bergstrom, CA., 2013. Computational prediction of drug solubility in lipid based formulation excipients. Pharm. Res. 30 (12), 3225–3237. https://doi.org/10.1007/s11095-013-1083-7.

13 O'Shea, JP, Faisal, W, Ruane-O'Hora, T, Devine, KJ, Kostewicz, ES, O'Driscoll, CM, et al., 2015. Lipidic dispersion to reduce food dependent oral bioavailability of fenofibrate: In vitro, in vivo and in silico assessments. Eur. J. Pharm. Biopharm. 96, 207–216. 10.1016/j.ejpb.2015.07.014.

14 Butler, J, Hens, B, Vertzoni, M, Brouwers, J, Berben, P, Dressman, J, et al., 2019. In vitro models for the prediction of in vivo performance of oral dosage forms: Recent progress from partnership through the IMI OrBiTo collaboration. Eur. J. Pharm. Biopharm. 136, 70–83. 10.1016/j.ejpb.2018.12.010.

15 Andreas, CJ, Rosenberger, J, Butler, J, Augustijns, P, McAllister, M, Abrahamsson, B, et al., 2018. Introduction to the OrBiTo decision tree to select the most appropriate in vitro methodology for release testing of solid oral dosage forms during development. Eur. J. Pharm. Biopharm. 130, 207–213. 10.1016/j.ejpb.2018.07.003.

16 Christiansen, ML, Müllertz, A, Garmer, M, Kristensen, J, Jacobsen, J, Abrahamsson, B, et al., 2015. Evaluation of the Use of Göttingen Minipigs to Predict Food Effects on the Oral Absorption of Drugs in Humans. J. Pharm. Sci. 104 (1), 135–143. https://doi.org/10.1002/jps.24270.

17 Henze, LJ, Koehl, NJ, O'Shea, JP, Kostewicz, ES, Holm, R, Griffin, BT, 2019. The pig as a preclinical model for predicting oral bioavailability and in vivo performance of pharmaceutical oral dosage forms: a PEARRL review. J. Pharm. Pharmacol. 71 (4), 581–602. https://doi.org/10.1111/jphp.12912.

18 Henze, LJ, Koehl, NJ, O'Shea, JP, Holm, R, Vertzoni, M, Griffin, BT, 2019. Toward the establishment of a standardized pre-clinical porcine model to predict food effects – Case studies on fenofibrate and paracetamol. Int. J. Pharm. 1, 100017 https://doi.org/10.1016/j.ijpx.2019.100017.

19 Dressman, JB, Vertzoni, M, Goumas, K, Reppas, C., 2007. Estimating drug solubility in the gastrointestinal tract. Adv. Drug Deliv. Rev. 59 (7), 591–602. https://doi.org/10.1016/j.addr.2007.05.009.

20 Merchant, HA, Afonso-Pereira, F, Rabbie, SC, Youssef, SA, Basit, AW., 2015. Gastrointestinal characterisation and drug solubility determination in animals. J. Pharm. Pharmacol. 67 (5), 630–639.

21 Henze, LJ, Koehl, NJ, Jansen, R, Holm, R, Vertzoni, M, Whitfield, PD, et al., 2020. Development and evaluation of a biorelevant medium simulating porcine gastrointestinal fluids. Eur. J. Pharm. Biopharm. 154, 116–126. https://doi.org/10.1016/j.ejpb.2020.06.009.

22 Mullertz, A, Reppas, C, Psachoulias, D, Vertzoni, M, Fatouros, DG., 2015. Structural features of colloidal species in the human fasted upper small intestine. J. Pharm. Pharmacol. 67 (4), 486–492. https://doi.org/10.1111/jphp.12336.

23 Riethorst, D, Baatsen, P, Remijn, C, Mitra, A, Tack, J, Brouwers, J, et al., 2016. An In-Depth View into Human Intestinal Fluid Colloids: Intersubject Variability in Relation to Composition. Mol. Pharm. 13 (10), 3484–3493. 10.1021/acs.molpharmaceut.6b00496.

24 Riethorst, D, Mols, R, Duchateau, G, Tack, J, Brouwers, J, Augustijns, P., 2016. Characterization of Human Duodenal Fluids in Fasted and Fed State Conditions. J. Pharm. Sci. 105 (2), 673–681. https://doi.org/10.1002/jps.24603.

25 Bennett-Lenane, H, Koehl, NJ, O'Dwyer, PJ, Box, KJ, O'Shea, JP, Griffin, BT, 2021 Jan. Applying Computational Predictions of Biorelevant Solubility Ratio Upon Self-Emulsifying Lipid-Based Formulations Dispersion to Predict Dose Number. J. Pharm. Sci. 110 (1), 164–175. https://doi.org/10.1016/j.xphs.2020.10.055.

26 Fagerberg, JH, Bergstrom, CA., 2015. Intestinal solubility and absorption of poorly water soluble compounds: predictions, challenges and solutions. Ther. Deliv. 6 (8), 935–959. https://doi.org/10.4155/tde.15.45.

27 Abrahamsson, B, McAllister, M, Augustijns, P, Zane, P, Butler, J, Holm, R, et al., 2020. Six years of progress in the oral biopharmaceutics area – A summary from the IMI OrBiTo project. Eur. J. Pharm. Biopharm. 152, 236–247. https://doi.org/10.1016/j.ejpb.2020.05.008.

28 Wiest, J, Saedtler, M, Bottcher, B, Grune, M, Reggane, M, Galli, B, et al., 2018. Geometrical and Structural Dynamics of Imatinib within Biorelevant Colloids. Mol. Pharm. 15 (10), 4470–4480. 10.1021/acs.molpharmaceut.8b00469.

29 Tran, T, Fatouros, DG, Vertzoni, M, Reppas, C, Müllertz, A., 2017. Mapping the intermediate digestion phases of human healthy intestinal contents from distal ileum and caecum at fasted and fed state conditions. J. Pharm. Pharmacol. 69 (3), 265–273. https://doi.org/10.1111/jphp.12686.

30 Fatouros, DG, Walrand, I, Bergenstahl, B, Mullertz, A., 2009. Colloidal structures in media simulating intestinal fed state conditions with and without lipolysis products. Pharm. Res. 26 (2), 361–374. https://doi.org/10.1007/s11095-008-9750-9.

31 Mullertz, A, Fatouros, DG, Smith, JR, Vertzoni, M, Reppas, C., 2012. Insights into intermediate phases of human intestinal fluids visualized by atomic force microscopy and cryo-transmission electron microscopy ex vivo. Mol. Pharm. 9 (2), 237–247. https://doi.org/10.1021/mp200286x.

32 Griffin, BT, Kuentz, M, Vertzoni, M, Kostewicz, ES, Fei, Y, Faisal, W, et al., 2014. Comparison of in vitro tests at various levels of complexity for the prediction of in vivo performance of lipid-based formulations: case studies with fenofibrate. Eur. J. Pharm. Biopharm. 86 (3), 427–437. 10.1016/j.ejpb.2013.10.016.

33 Fatouros, DG, Bergenstahl, B, Mullertz, A., 2007. Morphological observations on a lipid-based drug delivery system during in vitro digestion. Eur. J. Pharm. Sci. 31 (2), 85–94. https://doi.org/10.1016/j.ejps.2007.02.009.

34 Alskär, LC, Parrow, A, Keemink, J, Johansson, P, Abrahamsson, B, Bergström, CAS., 2019. Effect of lipids on absorption of carvedilol in dogs: Is coadministration of lipids as efficient as a lipid-based formulation? J. Control. Release 304, 90–100. https://doi.org/10.1016/j.jconrel.2019.04.038.

35 Al-Gousous, J, Tsume, Y, Fu, M, Salem, II, Langguth, P., 2017. Unpredictable Performance of pH-Dependent Coatings Accentuates the Need for Improved Predictive in Vitro Test Systems. Mol. Pharm. 14 (12), 4209–4219. 10.1021/acs.molpharmaceut.6b00877.

36 Löbenberg, R, Amidon, GL., 2000. Modern bioavailability, bioequivalence and biopharmaceutics classification system. New scientific approaches to international regulatory standards. Eur. J. Pharm. Biopharm. 50 (1), 3–12. https://doi.org/10.1016/s0939-6411(00)00091-6.

37 Mudie, DM, Murray, K, Hoad, CL, Pritchard, SE, Garnett, MC, Amidon, GL, et al., 2014. Quantification of Gastrointestinal Liquid Volumes and Distribution Following a 240 mL Dose of Water in the Fasted State. Mol. Pharm. 11 (9), 3039–3047. https://doi.org/10.1021/mp500210c.

38 Amidon, GL, Lennernas, H, Shah, VP, Crison, JR., 1995. A theoretical basis for a biopharmaceutic drug classification: the correlation of in vitro drug product dissolution and in vivo bioavailability. Pharm. Res. 12 (3), 413–420. https://doi.org/10.1023/a:1016212804288.

39 Butler, JM, Dressman, JB., 2010. The developability classification system: application of biopharmaceutics concepts to formulation development. J. Pharm. Sci. 99 (12), 4940–4954. https://doi.org/10.1002/jps.22217.